

# CASALS: an Adaptive Lidar and Spectrometry SmallSat for a NASA Explorer Mission

David Harding, Guangning Yang, Jeffrey Chen, Mark Stephen, Xiaoli Sun, David Durachka, Hui Li, Wei Lu, James Mackinnon, Travis Wise, Jon Ranson and Philip Dabney

All at: NASA Goddard Space Flight Center, 8800 Greenbelt Rd, Greenbelt, MD 20771, USA  
Email: david.j.harding@nasa.gov

## 1. Introduction

Continuation of laser altimeter observations of the Earth's land and ice sheet topography, sea ice thickness and vegetation structure, begun by NASA's ICESat, ICESat-2 and GEDI missions, is crucial for monitoring and predicting the response of the Earth's surface to climate and land cover change over decadal scales. We are developing an observing system, consisting of a highly efficient, adaptive lidar and a spectrometer, intended for a SmallSat mission later in this decade. The system could serve as the foundation for long-term monitoring of the vertical dimension, composition, and function of the Earth's surface in a series of moderate-cost satellites. The approach addresses three of the Explorer Observables recommended in the 2017 Earth Science Decadal Survey (Committee on the Decadal Survey 2017): ice elevation, snow depth and snow water equivalent, and ecosystem structure. It can also serve as a pathfinder for global mapping of Surface Topography and Vegetation (STV) and the Planetary Boundary Layer (PBL), the two recommended longer-term Incubation Observables.

### 1.1 Concurrent Artificially-intelligent Spectrometry and Adaptive Lidar System

The observing system, the Concurrent Artificially-intelligent Spectrometry and Adaptive Lidar System (CASALS), includes a lidar which can rapidly adapt the laser footprint locations across a 7km wide swath and a VNIR-SWIR spectrometer with a  $\geq 30$ km wide swath and 30m pixels. CASALS combines lidar and spectral imaging to merge height data with information about composition and function, thereby enabling new capabilities for characterizing the physical state of the Earth's surface and processes acting upon it. Real-time data analysis, utilizing deep learning models based on techniques such as Long-term Short-term and temporal convolutional networks, will enable autonomous lidar targeting. Use of deep learning enhanced tensor completion will enable software-defined compressive sensing to optimize the adaptive sampling patterns. We are using very large Goddard Lidar Hyperspectral Thermal (G-LiHT) airborne data sets for training and model development. On-board processing will also enable reduction of downlink data volume by intelligent data selection, product generation and compression optimized for land cover specific science and application objectives.

## 2. CASALS Sensors

### 2.1 Adaptive Lidar

The block diagram in Figure 1 depicts the high-level functions of the CASALS laser transmitter, receiver, and electronics assemblies. All functionality is based on highly efficient, compact, space-qualifiable components to minimize size, weight, and power to enable a SmallSat implementation. The laser transmitter is based on a state-of-the-art, high-efficiency, 1 micron, solid-state, pulsed laser operating at up to 120KHz, with a compact, photonic integrated circuit (PIC) seed laser and a Yb fiber power amplifier. The laser beam is scanned across a 7km wide swath using a novel passive approach, with no need for a mechanism. This is accomplished by wavelength tuning the seed laser at high-speed, over the range 1.020 and 1.045 microns, and transmitting the beam through a wavelength-to-angle dispersive grating (Figure 1). The receiver telescope will employ free-form optics to reduce its size and weight. In a standard ESPA SmallSat bus, the aperture diameter would be 0.4m. In an ESPA Grande SmallSat the aperture could be as large as 0.9m. Because there is no beam splitting, individual laser pulses are received sequentially. Filtering before the lidar detector is done to reduce solar background noise, rejecting sunlight outside the laser tuning range. Linear-mode, photon-sensitive detection will be done using a 2x64 pixel version of a 2x8 state-of-the-art, HgCdTe detector array developed by DRS,

Inc. in collaboration with NASA GSFC (Sun et al. 2019). Although the laser operates at rates up to 120KHz in our concept, each element of the array will only detect pulses at a maximum rate of 8KHz, thereby preventing cloud folding and enabling profiling of the entire atmospheric column. Using multiple digitizers, the detector's analog output will be recorded at high speed for surface altimetry waveforms and at lower speed for atmospheric cloud and aerosol distributions.

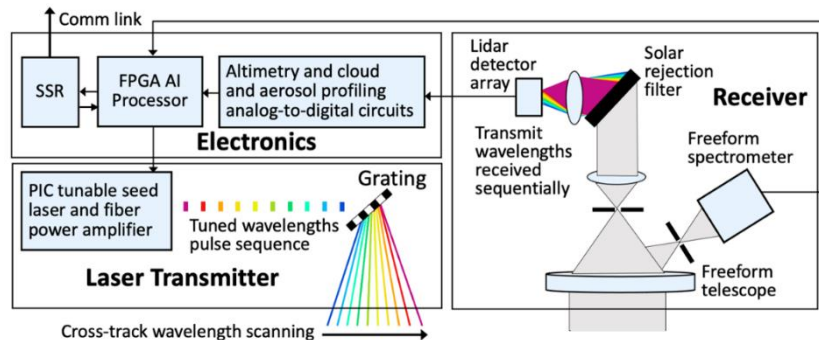


Figure 1: Block diagram of CASALS subsystems, major components and scanning method.

An accompanying, look-ahead thermal microbolometer (not shown) at 1km resolution will image a wide-swath to identify cloud-free areas day and night over land and ice sheets. Autonomous lidar targeting decisions in clear areas will be based on an on-board global land-cover map, spectral image analysis, prioritization of science and application objectives, and tasking uploads for critical dynamic events such as outlet glacier surges, active volcanoes, or ecosystem-damaging insect infestations. Targeting decisions and compressive sensing will be used to configure the adaptive beam scanning to best serve the objectives for a land cover type or event. Figure 2 depicts various configuration options.

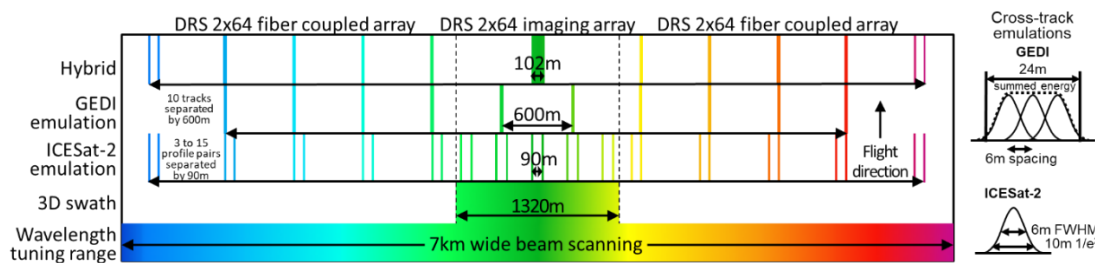


Figure 2: Example configurations of CASALS wavelength-tuned, cross-track beam locations, depicting 3D swath mapping, ICESat-2 and GEDI profile emulations, and a hybrid configuration.

Rapidly tuning the wavelength points 10m diameter ( $1/e^2$ ) footprints to any location separated by 6m across a 7km wide field-of-view (FOV). The DRS 2x64 pixel detector array will not be able to image the entire swath. Our concept is to image a central swath, up to 1,320m wide onto one array, achieving 3-D lidar swath mapping from space for the first time. A second array would be fiber coupled to specific locations across the receiver FOV, enabling continuity with the profile patterns of ICESat-2, with as many as 15 pairs of profiles separated by 90, and GEDI, with as many as 10 profiles separated by 600m. ICESat-2 emulation would use single footprint profiles to match that mission's  $\sim 10$ m footprints, whereas GEDI-emulation would use 3 profiles with 6m cross-track spacing to match that mission's 24m diameter footprints (Figure 2). Along-track footprint spacing can be rapidly changed, from overlapping to widely spaced by changing pulse-rate, to optimize footprint density depending on target height complexity.

The expected lidar performance has been predicted using a comprehensive modelling capability that extends models done for previous missions at Goddard (Sun et al 2013). The model includes more complete treatments of ranging error due to laser speckle, detector timing jitter, finite digitizer sampling and solar background noise. It also estimates the relative random error (RRE) of the surface reflectance measurement. Baseline modelling is for a laser transmitting 30 wavelengths at a total rate of 53KHz with 11W average optical power and a 0.4m receiver telescope, using six design cases developed for the ICESat-2 mission (1a: ice sheet interior, 4: outlet glacier, 7a: tropical flat with moderate and very dense

canopy covers, 9b: boreal hilly with sparse and dense canopy covers). Key performance factors are the number of detected photons and the RMS ranging error for single laser pulses and for 24 overlapping pulses, as well as the solar noise photon rate. The 24 pulses define either a 12m x 72m profile segment emulating the ICESat-2 data product or a 24m x 24m area emulating a GEDI footprint. For cases 1a and 4 profile segments, the predicted ranging errors are similar to those predicted pre-launch by the ICESat-2 project for that mission's photon-counting strong beam (0.01 and 0.13m, respectively). The very low noise DRS detector array, low solar background and the 500 to 600 predicted signal photons for GEDI-emulation vegetation waveforms (cases 7a and 7b), yields SNR levels typical of those acquired by high-pulse energy, full-waveform, large-footprint lidars of the type used by GEDI (Sun et al 2013). For ground topography in the vegetation design cases, the predicted single-footprint RMS ranging errors fall between the 0.5m threshold and 0.1m aspirational vertical accuracy goals identified in a study of the Decadal Survey STV Observable conducted for NASA (STV Study Team 2021), other than the very challenging 7a case with 99% canopy closure.

## 2.2 Imaging Spectrometer

Several design factors are being evaluated for the spectrometer. Those include swath width, wavelength range, band width, band sampling (continuous hyperspectral or discrete multispectral), optical design (traditional or free-form) and configuration with the lidar (sharing a telescope, separate telescopes on one satellite or separate satellites flying close in time on the same orbit path). The baseline is a traditional optical design developed for a GSFC forest-ecosystem SmallSat mission concept with a 30km swath and 21 narrow VNIR and SWIR bands optimized for vegetation function indices and atmospheric correction. Several additional bands would be added for characterization of snow and ice properties, including grain size, contaminant levels and water concentration. A more advanced spectrometer in development at GSFC is also being considered, with a 90km swath and full VNIR and SWIR spectrum, using free-form optics to dramatically reduce size and weight compared to traditional spectrometers.

## 3. Development Status

The CASALS lidar technologies are being developed and demonstrated in two steps. We are demonstrating the transmitter and receiver functions at 1.5 micron using high-maturity, in-hand components, and will range horizontally to calibration and natural targets over distances of about 1km. The electronics will use commercial National Instruments PIXe cards. Demonstration of this prototype is expected in late 2021, done in combination with commercial VNIR hyperspectral and SWIR multispectral cameras. Meanwhile, with industry and university partners, we are migrating the laser transmitter components to 1 micron, which is necessary to achieve the efficiencies needed for spaceflight use. That lidar and spectrometry system will be capable of operating at high altitudes, up to 20km. We are also migrating the data system to an FPGA processor which emulates the GSFC SpaceCube spaceflight processor architecture. Demonstration of this prototype is expected in late 2022.

## Acknowledgements

This work is being supported by the GSFC Radical Innovation Initiative, the NASA Earth Science Technology Office IIP and ACT programs and the NASA Small Business Innovation Research program.

## References

- Committee on the Decadal Survey for Earth Science and Applications from Space Space Studies Board, 2017, *Thriving on Our Changing Planet: A Decadal Strategy for Earth Observation from Space*, The National Academies Press, Washington, D.C.
- STV Study Team, 2021, *Observing Earth's Changing Surface Topography and Vegetation Structure: A Framework for the Decade*, NASA Surface Topography and Vegetation Incubation Study. National Aeronautics and Space Administration.
- Sun X, Abshire JB, McGarry JF, Neumann GA, Smith JC, Cavanaugh JF, Harding DJ, Zwally HJ, Smith DE and Zuber MT, 2013, Space Lidar Developed at the NASA Goddard Space Flight Center - The First 20 Years, *IEEE Journal of Selected Topics in Applied Earth Observations and Remote Sensing*, 6(3): 1660-1675.
- Sun X, Abshire JA, Krainak MA, Lu W, Beck JD, Sullivan III WW, Mitra P, Rawlings DM, Fields RA, Hinkley DA and Hirasuna BS, 2019, HgCdTe avalanche photodiode array detectors with single photon sensitivity and integrated detector cooler assemblies for space lidar applications, *Optical Engineering*, 58(6): Paper 067103.